Macromolecules

ARTICLE

pubs.acs.org/Macromolecules

Strain Hardening and Strain Softening of Reversibly Cross-Linked Supramolecular Polymer Networks

Donghua Xu*,† and Stephen L. Craig*,‡

†State Key Laboratory of Polymer Physics and Chemistry, Changchun Institute of Applied Chemistry, Chinese Academy of Sciences, Changchun 130022, P. R. China

‡Department of Chemistry and Center for Biologically Inspired Materials and Material Systems, Duke University, Durham, North Carolina 27708-0346, United States

Supporting Information

ABSTRACT: The large amplitude oscillatory shear behavior of metallo-supramolecular polymer networks formed by adding bis-Pd(II) cross-linkers to poly(4-vinylpyridine) (PVP) in dimethyl sulfoxide (DMSO) solution is reported. The influence of scanning frequency, dissociation rate of cross-linkers, concentration of cross-linkers, and concentration of PVP solution on the large amplitude oscillatory shear behavior is explored. In semidilute unentangled PVP solutions, above a critical scanning frequency, strain hardening of both storage moduli and loss moduli is observed. In the semidilute entangled regime of PVP solution, however, strain softening is observed for samples with faster cross-linkers ($k_d \sim 1450\ s^{-1}$), whereas strain hardening is observed for samples with slower cross-linkers ($k_d \sim 17\ s^{-1}$). The mechanism of strain hardening is attributed primarily to a strain-induced increase in the number of elastically active chains, with possible contributions from non-Gaussian stretching of polymer chains at strains approaching network fracture. The divergent strain softening of samples with faster cross-linkers in semidilute entangled PVP solutions, relative to the strain hardening of samples with slower cross-linkers, is consistent with observed shear thinning/shear thickening behavior reported previously and is attributed to the fact that the average time that a cross-linker remains detached is too short to permit the local relaxation of polymer chain segments that is necessary for a net conversion of elastically inactive to elastically active cross-linkers. These and other observations paint a picture in which strain softening and shear thinning arise from the same set of molecular mechanisms, conceptually uniting the two nonlinear responses for this system.

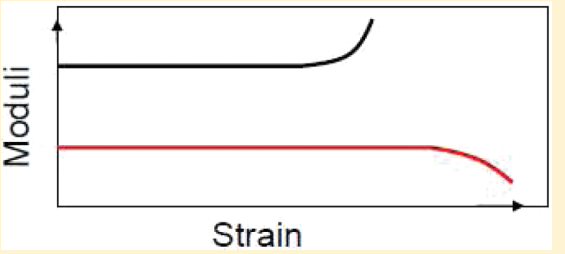

INTRODUCTION

Associative polymers have rich rheological behavior that fuels their use in a wide range of applications and motivates interest in the mechanisms that determine their behavior.[1−6] Their rheological properties can be categorized into two classes of viscoelastic response:[7] linear viscoelasticity, as normally measured by small amplitude oscillatory shear, and nonlinear viscoelasticity, such as that which occurs under high steady shear rate and large amplitude oscillatory shear.[7] In contrast to their linear rheological properties, the mechanisms underlying the nonlinear rheological properties of associative polymers vary from one system to another and are often unclear. As a result, extensive experimental and theoretical research has been devoted to the molecular origin of shear thickening and strain hardening of associative polymers.[8−18]

At the core of the visoelastic response of associative polymers is the reversible association itself, and our group has previously demonstrated a useful method of probing the contributions of molecular reversibility to the macroscopic rheological properties of supramolecular polymer networks.[18−21] The method takes advantage of steric effects at the *N*-alkyl positions of *N,C,N*-pincer Pd(II) and Pt(II) complexes[17] through which the dissociation rate of the cross-linkers can be changed by orders of magnitude independently of the association constant.[22] Recently, the steady shear behavior of the metallo-supramolecular polymer networks formed by these bis-Pd(II) cross-linkers and poly(4-vinylpyridine) (PVP) was reported (Figure 1).[18,21,23] The mechanism of shear thickening of samples in the semidilute unentangled regime and divergent shear thinning versus shear thickening of samples with identical structure but different cross-linker kinetics in the semidilute entangled regime were explored.[18,21,23] We found that shear thickening was dominated by a conversion of intrachain to interchain bound cross-linkers but that the competition between reassociation of dissociated cross-linkers and polymer chain diffusion contributed to the efficiency of the conversion process.[18,21,23] In this article, the large amplitude oscillatory shear (LAOS) behavior of the same metallo-supramolecular polymer networks is examined.

Received: June 20, 2011
Revised: August 17, 2011
Published: August 30, 2011

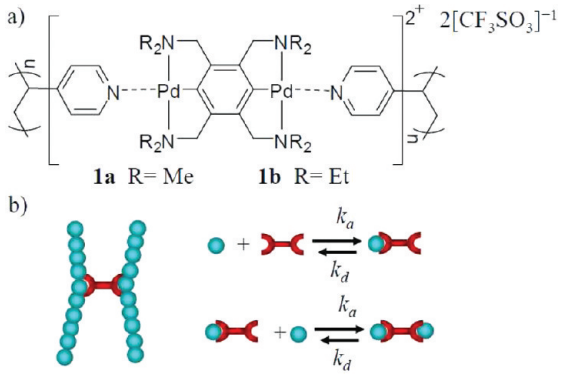

Figure 1. (a) Schematic picture of networks formed from poly(4-vinylpyridine) (PVP) chains and bis-Pd(II) cross-linkers (**1a** or **1b**). (b) Schematic picture of the kinetic parameters of the supramolecular interaction underlying network formation. Each pyridine unit in the PVP chain is represented by a bead. Reprinted from ref 27. Copyright 2011 American Chemical Society.

The LAOS experiments allow us to probe the strain hardening and/or strain softening behavior of the networks,[7,24,25] classes of nonlinear responses that are central to the behavior of materials under high-strain conditions but for which a detailed physical picture is often difficult to realize.[26] In analogy with the steady shear behavior, depending on the sample, strain hardening and/or strain softening are observed. The mechanisms underlying the LAOS response are explored, and the behavior is compared to the steady shear behavior previously reported.

EXPERIMENTAL SECTION

Materials. The bis-Pd(II) cross-linkers [2,3,5,6-tetrakis{(dimethylamino)methyl}phenylene-1,4-bis(palladiumtrifluoromethanesulfonate)] (**1a**) and [2,3,5,6-tetrakis{(diethylamino)methyl}phenylene-1,4-bis-(palladiumtrifluoromethanesulfonate)] (**1b**) were synthesized as reported elsewhere.[22] The binding thermodynamics and exchange kinetics of the metal−pyridine interactions have been characterized previously.[20] The equilibrium association constants (K_{eq}) and dissociation rate constants (k_d) for **1a**·pyridine in dimethyl sulfoxide (DMSO) at 25 °C are 29 M^{-1} and 1450 s^{-1}, respectively. K_{eq} and k_d for **1b**·pyridine in DMSO at 25 °C are 33 M^{-1} and 17 s^{-1}, respectively.[20] DMSO and poly(4-vinylpyridine) (PVP), with M_w = 60000 as reported by the producer, were used as received from Aldrich. The M_n and M_w of the PVP have been reported previously to be 22000 and 64300 g/mol (polydispersity index (PDI) = 2.92), respectively, in the literature.[28] We carried out an independent analysis of the specific PVP used in our experiments and obtained values of M_n = 33000 and M_w = 44500 g/mol (PDI = 1.35).[23]

Sample Preparation. Samples were prepared by mixing PVP solutions with cross-linker solutions. Details of the sample preparation can be found in a previous paper.[18] The concentration of cross-linkers in the samples varied from 1% to 5% (ratio of Pd atoms to N atoms in the pyridine units of the PVP), all of which are above the critical concentration to form a gel (shown previously to be approximately 0.8% for ∼0.10 g/mL PVP/DMSO solutions).[29] The concentration of PVP in the samples varies from 0.08 (semidilute unentangled regime) to 0.27 g/mL (semidilute entangled regime). Details about the concentration regimes of the PVP/DMSO solution have been characterized previously, and the critical concentration of entanglement at 25 °C is 0.155 g/mL.[23] Concentrations are often denoted with a "∼" to reflect the slight variation between samples made with cross-linker **1a** vs **1b**; see the Supporting Information for details.

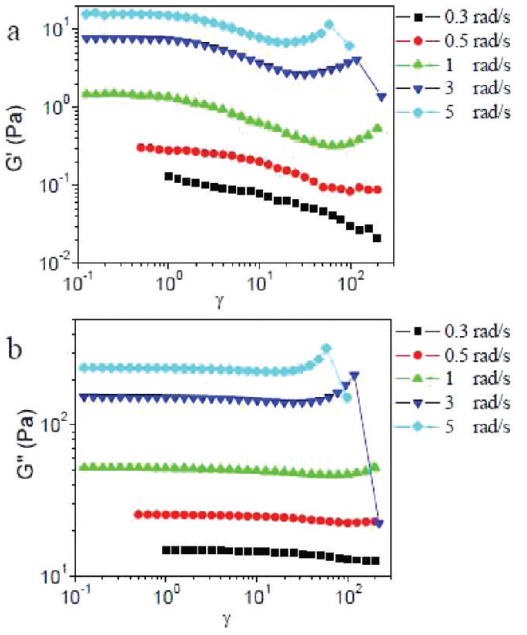

Figure 2. Storage modulus (G') and loss modulus G'' versus strain (γ) for a sample with 5% **1a** in ∼0.11 g/mL PVP during strain sweep experiments at different scanning frequencies.

Rheological Measurements. Rheological experiments were carried out at 25 °C. Data were obtained by using an AR G2 rheometer (TA Instruments) with cone−plate geometry (diameter of 20 mm, cone angle of 2°, truncation height of 49 μm). Strain sweep experiments were performed at different scanning frequencies. Oscillatory frequency sweeps from 10 to ∼30 rad/s were carried out at strains that spanned from the linear rheological region to the nonlinear rheological region for samples with **1b**.

The inertia and torque of the AR-G2 rheometer (stress controlled rheometer) must be calibrated carefully in order to measure the small values of the storage modulus (G') of a low viscosity fluid at high frequency, where the measured torque is the sum of the sample torque and inertial torque.[30] Slight deviations in the inertial torque can cause significant variations in the derived sample torque. A useful parameter to monitor the effect of inertia, and one we employ here, is the measured (raw) phase angle (δ_m). If the inertia shifts the phase angle, δ_m will be larger than the sample's phase angle (δ_s). Measurements with a raw phase angle below 170° can be calibrated,[30] but to avoid the influence of inertial effects on the nonlinear rheological properties of samples in this work, only the data for which $\delta_m = \delta_s$ are used in this article. This restriction limits the range of available scanning frequencies for the strain sweep experiments, especially for samples with low viscosity.[30]

Data Treatment. At small strain amplitudes, when the response is linear, the material is commonly characterized by the storage modulus (G') and loss modulus (G''), as determined from the components of the time dependent stress $\sigma(t)$ in phase with time dependent strain $\gamma(t)$ and time dependent strain rate $\dot{\gamma}(t)$, respectively, as follows:[31]

$$\gamma(t) = \gamma_0 \sin(\omega t) \quad (1)$$

$$\dot{\gamma}(t) = \gamma_0 \omega \cos(\omega t) \quad (2)$$

$$\sigma(t) = \sigma_0 \sin[\omega t + \delta] = \gamma_0[G' \sin(\omega t) + G'' \cos(\omega t)] \quad (3)$$

where γ_0 is the strain amplitude, ω is frequency, t is time, $\gamma_0\omega$ is the strain rate amplitude, σ_0 is amplitude of the stress, and δ is the phase angle.

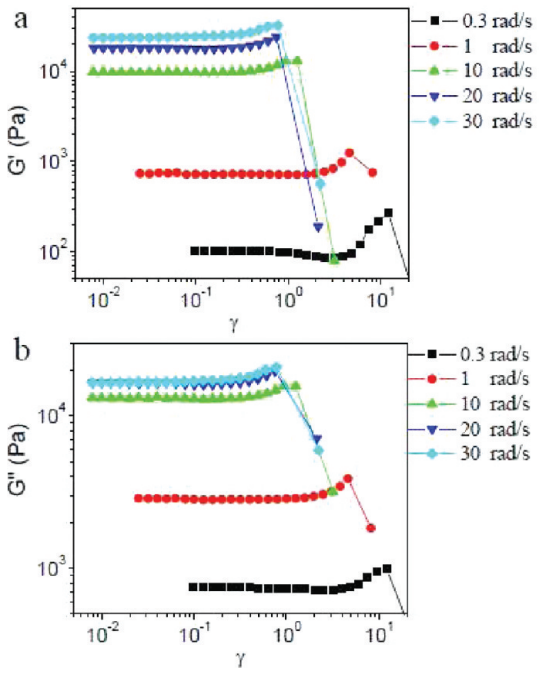

Figure 3. Storage modulus (G') and loss modulus (G'') versus strain (γ) for a sample with 5% **1b** in ~0.11 g/mL PVP during strain sweep experiments at different scanning frequencies.

The strain amplitude γ_0 can be increased systematically to enter the nonlinear viscoelastic regime, resulting in a LAOS test. The linear storage moduli (G') and loss moduli (G'') are not uniquely defined once the material response becomes nonlinear[24] since a nonlinear stress response is not a single-harmonic sinusoid. Nonetheless, apparent values of G' and G'' have proven useful as a framework upon which to discuss nonlinear rheological properties,[14,32−34] and we adopt that practice here.

If the periodic stress response $\sigma(t)$ is plotted against $\gamma(t)$ (Lissajous−Bowditch curves), a linear viscoelastic response appears as an ellipse that contains two mirror planes (the major and minor axes of the ellipse), whereas a nonlinear viscoelastic response is characterized by Lissajous−Bowditch curves that deviate from ellipticity.[24] For example, Lissajous−Bowditch curves are not elliptical when secondary flow, wall slip, or non-Gaussian stretching of polymer chains takes place in the samples.[24,35,36] The Lissajous−Bowditch curves are used here to further characterize the details of the strain sweep behavior, especially during strain hardening or strain softening, and their use complements analyses based merely on G' and G''.

RESULTS

Strain Sweep Results in the Semidilute Unentangled Regime. *Influence of Scanning Frequency.* In Figure 2, the influence of the scanning frequency on the strain sweep behavior of ~0.11 g/mL PVP with 5% **1a** is shown. When the scanning frequency is 0.3 or 0.5 rad/s, substantial strain softening (modulus decreases with increasing strain, γ) is observed in G', while G'' remains nearly constant across the experimentally accessible range of γ. As the scan frequency is increased from 1 rad/s to 5 rad/s, G' is first constant, then decreases with increasing γ, and then increases at larger γ. G'' is constant at small strain and shows strain hardening (modulus increases with increasing γ) at larger strain. At 3 rad/s and 5 rad/s, a dramatic decrease in modulus at high γ is observed that corresponds to the

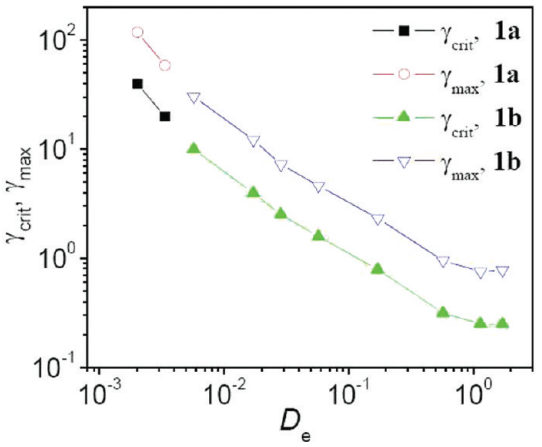

Figure 4. Critical strain (γ_{crit}) and maximum strain (γ_{max}) during strain hardening as a function of the Deborah number (D_e) for samples with 5% **1a** or 5% **1b** in ~0.11 g/mL PVP during strain sweep experiments at different scanning frequencies. Lines are provided to guide the eye.

fracture of the network and/or ejection of the sample from the geometry.[18] In this article, we do not focus on this fracture behavior further. Increasing the scanning frequency to above 10 rad/s causes the raw phase angle to become larger than the sample phase angle, meaning that inertia starts to affect the experimental results,[30] and these data are, therefore, omitted from further consideration.

The initial strain softening regime of ~0.11 g/mL PVP with 5% **1a** at low frequency is analyzed further by the raw strain sweep data. Lissajous−Bowditch curves of ~0.11 g/mL PVP with 5% **1a** in the strain softening regime are elliptical (Figure S1 in the Supporting Information), indicating a single-harmonic sinusoidal stress response in the strain-softened regime and ruling out substantial non-Gaussian stretching of polymer chains (consistent with expectations for behavior at low strains) for which the Lissajous−Bowditch curves would not be elliptical.[24] The mechanism behind the strain softening of G' at low frequency, during which G'' remains nearly constant, is not further explored in this article.

Strain sweep results of ~0.11 g/mL PVP with 5% of the slower cross-linker **1b** at different scanning frequencies are shown in Figure 3. Strain hardening of G' and G'' is observed when the scan frequency is as low as 0.3 rad/s, whereas no strain hardening is observed for the comparable **1a** network under those conditions (Figure 2). In Figure 3, ~0.11 g/mL PVP with 5% **1b** also shows some strain softening in G' prior to strain hardening at 0.3 rad/s, and the Lissajous−Bowditch curves are elliptical in the strain softening regime (Figure S2 in the Supporting Information; the Lissajous−Bowditch curves of ~0.11 g/mL PVP with 5% **1b** during strain hardening will be discussed in detail in the next section). During the strain softening of G', G'' is nearly constant (as seen in the **1a** networks), and the phase angle increases. Inertial contributions preclude analysis of data at scanning frequencies above 50 rad/s.

As seen in Figure 2, for samples with 5% **1a**, the value of critical strain (γ_{crit}, defined by the onset of strain hardening) or the maximum strain without network fracture during strain hardening (γ_{max}), decreases with increasing scanning frequency from 1 rad/s to 5 rad/s (Figure 2b). For samples with 5% **1b**, this trend between γ_{crit} (or γ_{max}) and the scanning frequency is also observed with the increase of scanning frequency from 0.3 rad/s

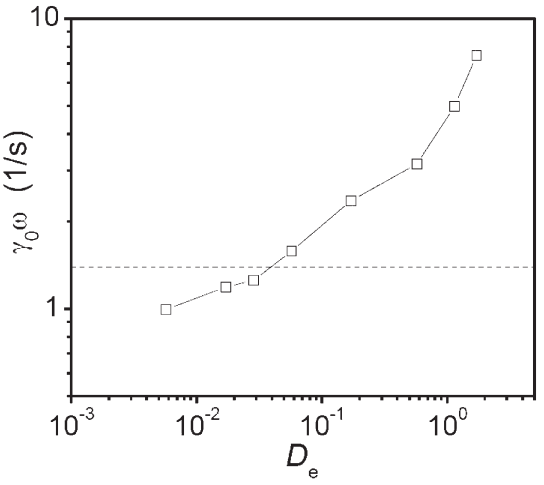

Figure 5. Strain rate amplitude ($\gamma_0\omega$) at the critical strain during strain hardening versus the Deborah number (D_e) for samples with 5% **1b** in ~0.11 g/mL PVP during strain sweep experiments at different scanning frequencies. The critical shear rate for the shear thickening of 5% **1b** in ~0.11 g/mL PVP is given by the dashed line ($\dot{\gamma}_{crit}$ = 1.4 s^{-1}).[18]

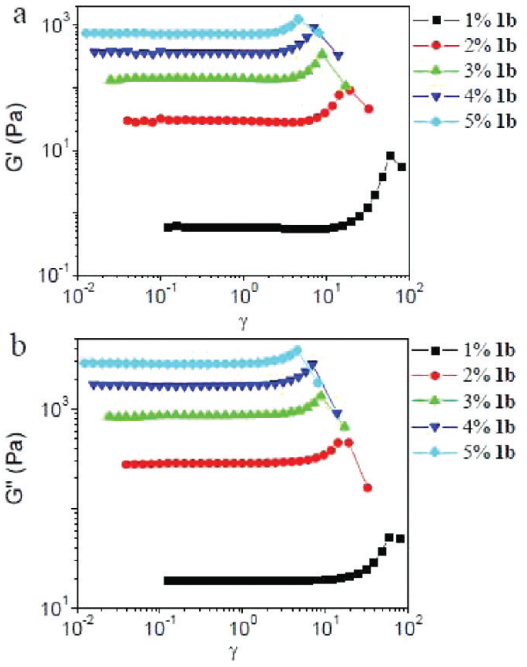

Figure 6. Storage (G') and loss (G'') moduli versus strain (γ) for samples with different concentrations of **1b** in a ~0.11 g/mL PVP solution. Scanning frequency is 1 rad/s.

to 10 rad/s, but the values of γ_{crit} and γ_{max} during strain hardening are almost the same from 20 rad/s to 30 rad/s (Figure 3). We also notice that, at 1 rad/s, the value of γ_{crit} and γ_{max} for ~0.11 g/mL PVP with 5% **1a** is much bigger than for that with 5% **1b**. Because the structure of **1a**·PVP and **1b**·PVP networks is effectively identical,[18−20] the different trends as a function of scanning frequency are attributed to the different relaxation times (τ) of the networks. The characterization of the apparent relaxation time (τ) of ~0.11 g/mL PVP with 5% **1a** or 5% **1b** in the linear regime are shown in Figure S3 in the Supporting Information. The apparent relaxation times (τ) of ~0.11 g/mL PVP with 5% **1a** or 5% **1b** are determined to be 6.7×10^{-4} s and 5.7×10^{-2} s, respectively.

We use the Deborah number ($D_e = \omega\tau$)[37] to interpret the strain sweep results in Figures 2 and 3. The relationship of γ_{crit} and γ_{max} to D_e for ~0.11 g/mL PVP with 5% **1b** (0.1 − 30 rad/s) and for ~0.11 g/mL PVP with 5% **1a** (3 − 5 rad/s) is shown in Figure 4. When $D_e < 1$, γ_{crit} and γ_{max} decrease as the scanning frequency is increased. When $D_e > 1$, γ_{crit} and γ_{max} remain nearly constant as a function of scanning frequency. From Figure 4, we also see that the values of γ_{crit} and γ_{max} for samples with **1a** or **1b** fall on the same master curves. This behavior is consistent with the scaling relationships reported previously for this system under linear oscillatory frequency sweep and steady shear[18,20,27] and verifies that the structures of samples with **1a** or **1b** are similar.

Similar dependencies of γ_{crit} and γ_{max} on D_e have been reported previously.[24,33,34] Tung et al. examined the strain hardening of lecithin/SDC reverse worms, and observed that when $D_e < 1$, γ_{crit} and γ_{max} decrease as the scanning frequency is increased.[34] Erk et al. observed that when $D_e > 1$, the onset of strain hardening in physical networks of triblock copolymers occurs at a similar value of strain.[33] The Deborah number measures the amount of elasticity,[24,38] and when the scanning frequency (ω) during strain sweep is smaller than the crossover frequency (ω_c) of G' and G'' (obtained from frequency sweep measurements), $D_e < 1$ and $G' < G''$, that is, the fluid is predominantly viscous. When $D_e > 1$, $G' < G''$ and the fluid is predominantly elastic,[38] Ewoldt et al. reported that at low scanning frequency ($D_e < 1$), the viscous nonlinearities during strain sweep become apparent near a Weissenberg number (W_i, $W_i = \gamma_0\omega\tau$) of close to 1.[24] As the strain rate amplitude ($\gamma_0\omega$) is analogous to the shear rate of steady shear experiments, the nonlinearities of a fluid during strain sweep with $D_e < 1$ implies a connection to nonlinear steady shear behavior, to which we return later in the article (Figure 5). Similar nonlinear behavior is observed at higher frequency ($D_e > 1$) (Figure 5) when the fluid is dominated by elasticity; the nonlinear regime during strain sweep was also found by Ewoldt et al. to be triggered at a critical strain amplitude.[24]

We note here that the maximum D_e number explored in this work is about 2 because of the experimental limitations on the range of scanning frequency. Wang's group reported that the large amplitude oscillatory shear (LAOS) behavior of a polymeric liquid at $D_e \gg 1$ can show more complex behavior such as wall slipping and/or shear banding.[39,40] We do not think that the strain hardening and strain softening behaviors are of interest to us in this work, which occur at $D_e < 3$, are related to wall slip and/or shear banding, which generally take place at much higher D_e.[39,40] Mechanistic probes of the behavior, discussed below, support this supposition.

Relationship Between Strain Hardening and Shear Thickening. Bossard et al. have compared the shear thickening effect (shear-induced viscosity enhancement) during steady shear experiments and the strain hardening of G' during strain sweep experiments in the context of a polyampholyte solution.[41] It was reported that the critical strain rate amplitude during strain hardening (~ 0.25 s^{-1}) is comparable to that of the critical shear rate for shear thickening (0.2 s^{-1}) obtained in a steady shear flow, and it was reasoned that strain hardening is related to the shear-thickening behavior.[41]

We, therefore, compare the critical strain rate amplitude ($\gamma_0\omega$) during the onset of strain hardening, taken at different

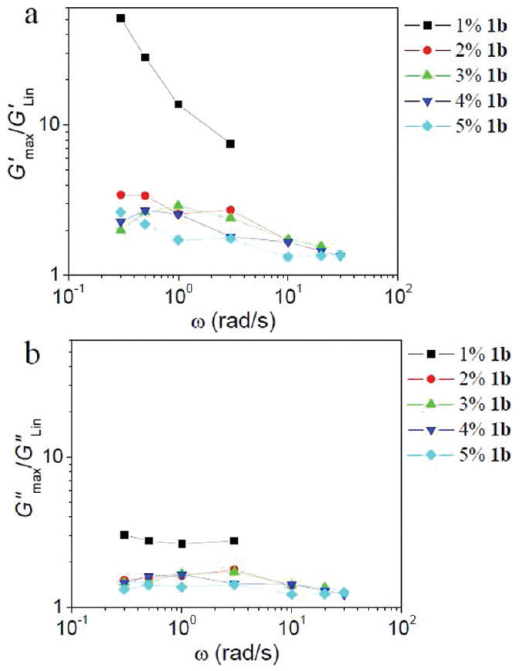

Figure 7. Degree of strain hardening in G' (a) and G'' (b) versus the scanning frequency (ω) for ~0.11 g/mL PVP with different concentrations of **1b** during strain sweep experiments at different scanning frequencies.

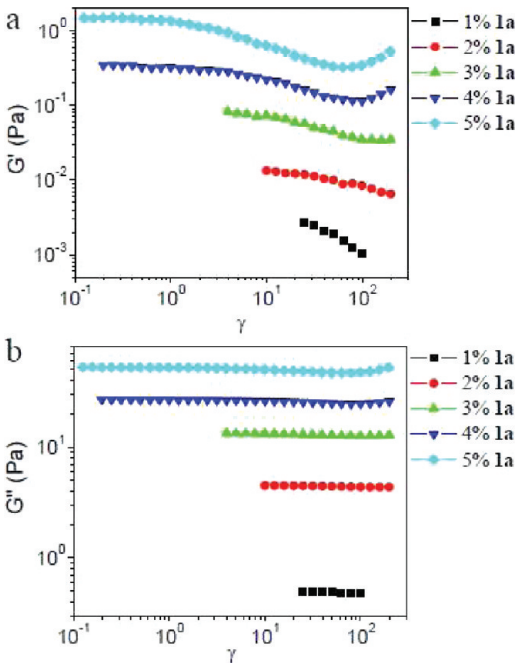

Figure 8. Storage modulus (G') and loss modulus (G'') versus strain (γ) for samples with different concentrations of **1a** in a ~0.11 g/mL PVP solution. Scanning frequency is 1 rad/s.

scanning frequencies for ~0.11 g/mL PVP with 5% **1b**, to the critical shear rate of the samples during steady shear ($\dot{\gamma}_{crit}$), previously reported to be 1.4 s^{-1}.[18] As shown in Figure 5, the critical strain rate amplitude ($\gamma_0\omega$) is close to the critical shear rate during steady shear when $D_e < 1$. This is consistent with Bossard et al.'s work and with our expectation, as stated above. The critical strain rate amplitude ($\gamma_0\omega$), however, is not a constant; the value of $\gamma_0\omega$ increases with increasing scanning frequency. The variance may reflect the fact that, during a strain sweep, the strain rate ranges from zero to the strain rate amplitude over each cycle of a dynamic oscillatory measurement.[31] This condition differs from the constant shear rate during steady shear experiments,[31] and the similarity in values is best taken semiquantitatively only. As D_e increases, we observe that the critical strain rate amplitude ($\gamma_0\omega$) increases, until the onset of nonlinearities of the fluid during strain sweep with $D_e > 1$ is several times larger than that at low D_e. Given the aforementioned uncertainty due to a variable strain rate in the oscillatory experiment, we are reluctant to try and interpret this trend. Although the absolute value belies a direct relationship with nonlinear steady shear behavior, the continuity in the trend shown in Figure 5 suggests that even in systems for which the strain sweep and steady shear onsets are substantially different, the two effects might originate from the same dynamics and mechanism.

Influence of Cross-Linker Concentration. In Figure 6, the strain sweep data at 1 rad/s are shown for ~0.11 g/mL PVP with different concentrations of **1b**. All of the samples exhibit strain hardening, and the values of γ_{crit} and γ_{max} decrease with increasing concentration of **1b**.

The degree of strain hardening is defined as the ratio between the maximum value of a modulus (either G'_{max} or G''_{max}) during strain hardening and the constant value of that modulus in the linear regime (G'_{Lin} and G''_{Lin}). In Figure 7, the degree of strain hardening (for both G' and G'') for different concentrations of **1b** is shown as a function of scanning frequency. The degree of strain hardening for both G' and G'' is greatest for the sample with 1% **1b**, whereas the degree of strain hardening is relatively independent of the concentration of **1b** from 2% to 5%. As seen in Figure 7, G'_{max}/G'_{Lin} is larger than G''_{max}/G''_{Lin}. This phenomenon is connected to the change of the phase angle during strain hardening, as discussed further below.

In Figure 8, strain sweep data for the **1a**·PVP networks (~0.11 g/mL PVP, 1 rad/s) with different concentrations of **1a** are shown. For samples with concentrations of **1a** from 1% to 3%, strain softening but no strain hardening in G' is observed across the range of strains accessed, whereas G'' is essentially constant; no strain hardening is observed across the experimentally accessible range. For samples with concentrations of **1a** of 4% or 5%, strain hardening is observed in G' and G''. The trends in γ_{crit} (or γ_{max}) as a function of concentration of **1a** are more complex than those for samples made with **1b** (Figure 6).

Influence of PVP Concentration on Strain Sweep Results. In Figures 9 and 10, strain sweep results in different concentrations of PVP solution are shown (scanning frequency is 1 rad/s) for samples with 5% **1a** or 5% **1b**, respectively. When the PVP concentration is below the critical concentration of entanglement (~0.155 g/mL),[23] strain hardening in both G' and G'' is observed for samples with both **1a** or **1b**. When the PVP concentration is above the critical entanglement concentration, however, samples with 5% **1a** show only strain softening in both G' and G'' (and, accordingly, in the complex modulus $|G^*| = (G'^2 + G''^2)^{1/2}$) (Figure 9).[31] This behavior contrasts with that of the samples made with 5% **1b** for which strain hardening in G' is observed from 0.159 g/mL to 0.190 g/mL PVP (Figure 10a), and strain hardening in G'' is observed at all concentrations examined (Figure 10b). All samples with 5% **1b** in the semidilute entangled regime show strain hardening in $|G^*|$.

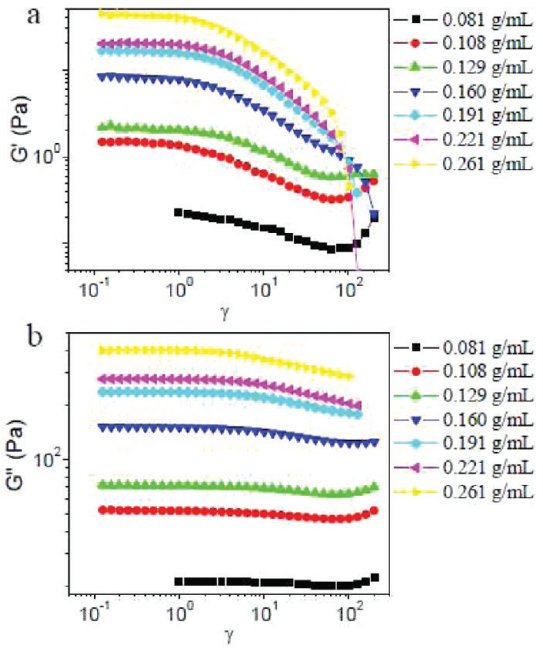

Figure 9. Storage (G') and loss (G'') moduli versus strain (γ) for samples with 5% **1a** in different concentrations of PVP solution. Scanning frequency is 1 rad/s.

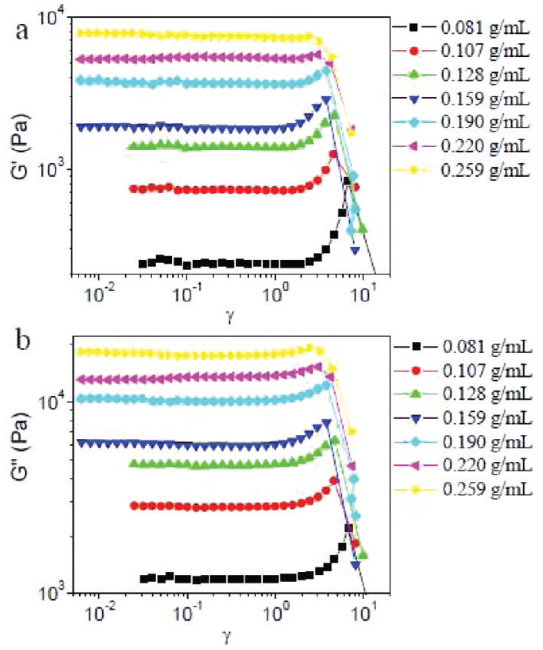

Figure 10. Storage (G') and loss (G'') moduli versus strain (γ) for samples with 5% **1b** in different concentrations of PVP solution. Scanning frequency is 1 rad/s.

These results are reminiscent of the divergent shear thinning/thickening behavior of the entangled **1**·PVP solutions reported previously,[21,23] suggesting that physical entanglement of PVP chains has an influence on the LAOS behavior. This observation motivates an examination of the strain sweep properties in the semidilute entangled regime.

Strain Sweep Results in the Semidilute Entangled Regime. *Influence of Scanning Frequency.* In Figure 11, the strain sweep

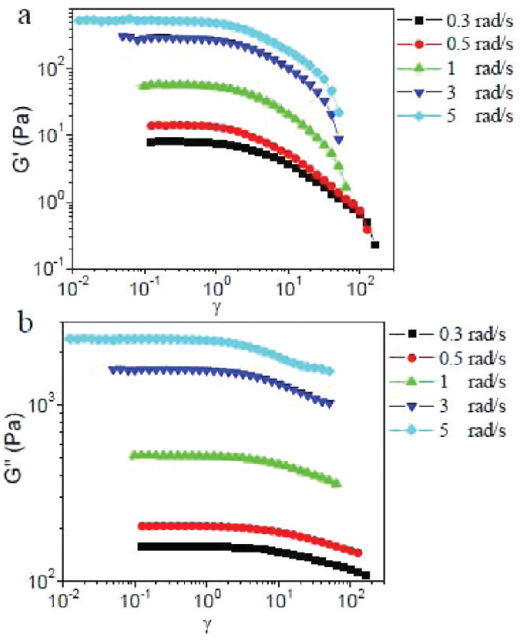

Figure 11. Storage (G') and loss (G'') moduli versus strain (γ) for samples with 5% **1a** in 0.261 g/mL PVP during strain sweep experiments at different scanning frequencies.

data of 0.261 g/mL PVP with 5% **1a** at different scanning frequencies are shown. As the scanning frequency is increased from 0.3 rad/s to 5 rad/s, 0.261 g/mL PVP with 5% **1a** always shows strain softening. These results contrast with that of the ∼0.11 g/mL PVP (semidilute unentangled regime) with 5% **1a** (Figure 2) for which strain hardening in G' and G'' is observed above 1 rad/s. Lissajous−Bowditch curves of 0.261 g/mL PVP with 5% **1a** in the strain softening regime appear as ellipses at scanning frequencies from 0.3 rad/s to 5 rad/s (Figures S4−S5 in the Supporting Information), again ruling out a substantial amount of non-Gaussian stretching of polymer chains.[24]

Shown in Figure 12 are the strain sweep data for 0.259 g/mL PVP with 5% **1b** at different scanning frequencies. As scanning frequency is increased from 0.3 rad/s to 1 rad/s, no strain hardening in G' is observed, in contrast to the strain hardening of G' for ∼0.11 g/mL PVP (semidilute unentangled regime) with 5% **1b**. For 0.259 g/mL PVP with 5% **1b** from 0.3 rad/s to 1 rad/s, strain hardening in G'' is still observed, and the complex moduli ($|G^*|$) still show strain hardening with the increasing of strain. The value of G''_{max}/G''_{Lin} and $|G^*_{max}|/|G^*_{Lin}|$ are around 1.1. Under 0.3 rad/s and 1 rad/s, the phase angle increases with strain in the nonlinear regime. With a further increase of scanning frequency to values from 10 to 30 rad/s, 0.259 g/mL PVP with 5% **1b** shows strain hardening in G' and G'', and the phase angle decreases with strain during strain hardening. Although the degree of strain hardening in G' is a little larger than the degree of strain hardening in G'', the values of G'_{max}/G'_{Lin} and G''_{max}/G''_{Lin} are both around 1.1.

Influence of Cross-Linker Concentration. In Figure 13, the strain sweep data of ∼0.27 g/mL PVP with different concentrations of **1a** at 1 rad/s are shown. As the concentration of **1a** increases from 1% to 5%, strain softening is observed in G' and G''. The concentration of **1a** does not have much influence on the strain softening of ∼0.27 g/mL PVP.

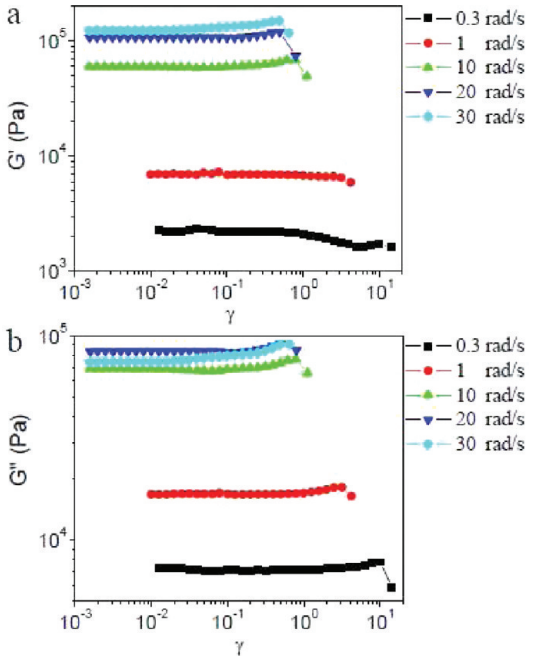

Figure 12. Storage (G') and loss (G'') moduli versus strain (γ) for samples with 5% **1b** in 0.259 g/mL PVP during strain sweep experiments at different scanning frequencies.

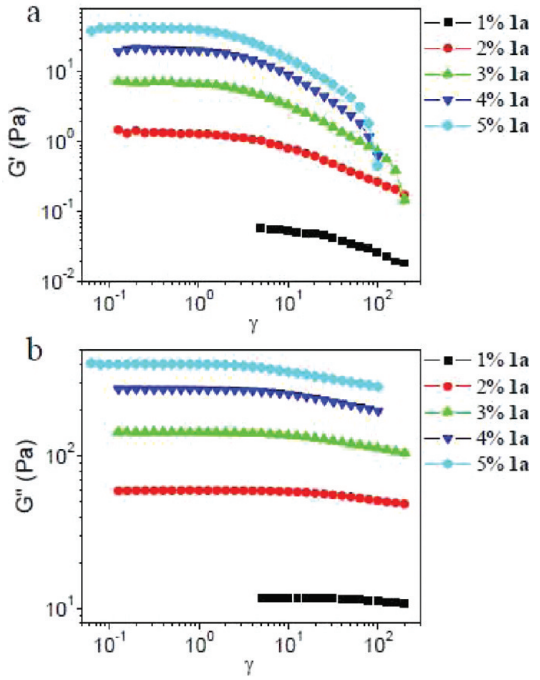

Figure 13. Storage (G') and loss (G'') moduli versus strain (γ) for samples with different concentrations of **1a** in a ~0.27 g/mL PVP solution. Scanning frequency is 1 rad/s.

The strain sweep data for ~0.26 g/mL PVP with different concentrations of **1b** at 1 rad/s are shown in Figure 14. Strain hardening is observed in G' for samples with 1% and 2% **1b**, and the phase angle decreases during strain hardening. For samples with concentrations of **1b** from 3% to 5%, no strain hardening in

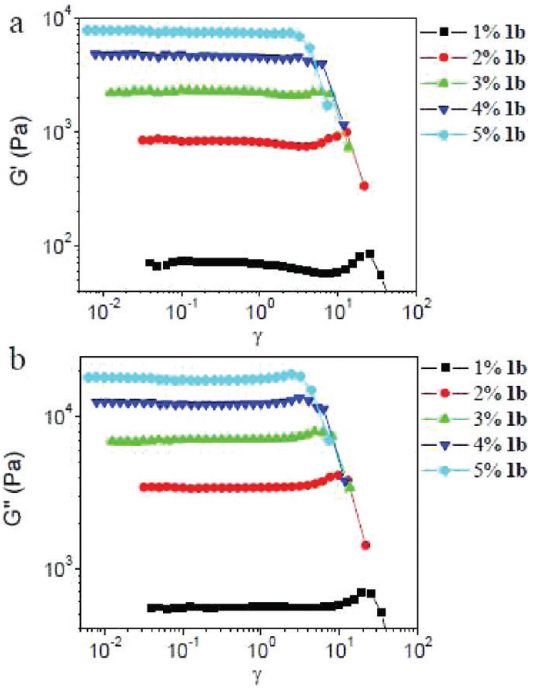

Figure 14. Storage (G') and loss (G'') moduli versus strain (γ) for samples with different concentrations of **1b** in a ~0.26 g/mL PVP solution. Scanning frequency is 1 rad/s.

G' is observed in the experimental range; the phase angle increases with strain in the nonlinear regime, and strain hardening in G'' (and $|G^*|$) is observed for all samples with **1b.**

Comparing the data in Figure 10 to that in Figure 14, we see that the concentration of the PVP solution and concentration of **1b** both affect the strain sweep results in the semidilute entangled regime. The fraction of elastically active chains increases with concentration of PVP and concentration of **1b**,[23] and the results here suggest that the fraction of elastically active chains influences the strain sweep behavior in a manner similar to that observed previously in the steady shear behavior.[23]

DISCUSSION

Mechanism of Strain Hardening. Proposed mechanisms of strain hardening for polymer networks fall into either of the two following main categories: one is strain-induced nonlinear high tension along chains that are stretched beyond the Gaussian range,[2,14,15,32,33] and the other is the strain-induced transformation of intrachain cross-linking to interchain cross-linking.[12,34,41] Regardless of the strain hardening mechanism, the degree of strain hardening of storage moduli (G'_{max}/G'_{Lin}) and loss moduli (G''_{max}/G''_{Lin}) can be expressed as[31]

$$G'_{max}/G'_{Lin} = (|G^*_{max}|/|G^*_{Lin}|)(\cos \delta_{max}/\cos \delta_{Lin}) \quad (4)$$

$$G''_{max}/G''_{Lin} = (|G^*_{max}|/|G^*_{Lin}|)(\sin \delta_{max}/\sin \delta_{Lin}) \quad (5)$$

where $|G^*_{Lin}|$ and $|G^*_{max}|$ are the complex moduli, and δ_{Lin} and δ_{max} are the phase angle in the linear regime and at the maximum strain during strain hardening, respectively. From eqs 4 and 5, we get

$$G'_{max}/G'_{Lin} = (G''_{max}/G''_{Lin})(\tan \delta_{Lin}/\tan \delta_{max}) \quad (6)$$

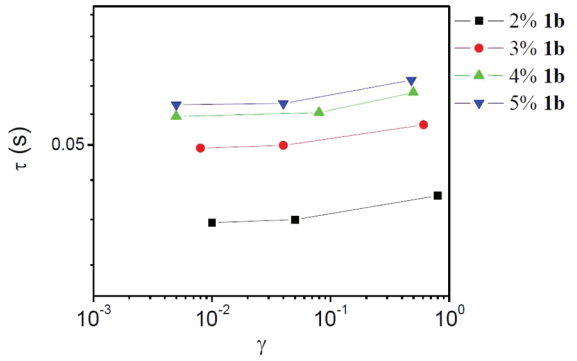

Figure 15. Apparent relaxation time (τ) of ~0.11 g/mL **1b**·PVP versus applied strain (γ) during an oscillatory frequency sweep from 10 to 30 rad/s.

Since a non-Gaussian stretching stress response is not a single-harmonic sinusoid, the periodic stress response $\sigma(t)$ versus $\gamma(t)$ (Lissajous−Bowditch curves) will cease to be elliptical in the strain hardening regime if strain hardening is caused by non-Gaussian stretching.[24] Another signature of non-Gaussian stretching arises from the partial rupture of the network that generally accompanies overstretching.[15] The observable consequence of the rupture is that δ_{max} is generally larger than δ_{Lin}, as was observed, for example, in work reported by Ma et al.[42] As $|G^*_{max}| / |G^*_{Lin}| > 1$, the fact that $\delta_{max} > \delta_{Lin}$ means that G'' will always show strain hardening under conditions of non-Gaussian overstretching, according to eq 5. On the other hand, G' (eq 4) may exhibit either strain hardening or softening, depending on the difference between δ_{max} and δ_{Lin}.[42] When G' also strain hardens, however, the degree of strain hardening in G'' is larger than the degree of strain hardening of G', according to eq 6. These relative strain hardening behaviors of G' and G'' have been reported previously for polymer networks[32,33] and tied to the non-Gaussian stretching of polymer chains in the strain hardening regime.[33] Under this mechanism of strain hardening, the relaxation time of the network (τ) is expected to decrease because of the partial break of the network under non-Gaussian stretching, as observed in Séréro et al.'s experimental work.[15]

In contrast, if strain hardening results from an increase in the number of elastically active chains, more energy is stored relative to that dissipated, and therefore, δ_{max} should be smaller than δ_{Lin}. According to eqs 4 and 5, then, $\delta_{max} < \delta_{Lin}$ means that G' will always show strain hardening, and G'' might show strain hardening or softening, depending on the difference between δ_{max} and δ_{Lin}. Furthermore, if G'' strain hardens, $\delta_{max} < \delta_{Lin}$ implies that the degree of strain hardening in G'' is smaller than the degree of strain hardening in G' (eq 6). Under this mechanism, the relaxation time of the network (τ) should increase because of the larger number of elastically active chains.[18] The relationship between τ during strain hardening and the degree of strain hardening in G' and G'' are discussed in the context of a single Maxwell model in the Supporting Information,[20] but briefly, τ is expected to increase if G'_{max}/G'_{Lin} is larger than G''_{max}/G''_{Lin}. This consequence is consistent with the decreasing of the phase angle during strain hardening, as discussed above. Finally, the time dependent stress response should still be a single-harmonic sinusoid during strain hardening, i.e., the Lissajous−Bowditch curves are still elliptical.[24]

The mechanism of strain hardening (non-Gaussian stretching vs increase in elastically active chains) can be distinguished by the following: (1) the change in τ during strain hardening; (2) the change in the phase angle during strain hardening; and (3) the shape of the Lissajous−Bowditch curves. We consider the change in τ, shown in Figure 15 as a function of applied strain for ~0.11 g/mL PVP with concentrations of **1b** from 2−5% (the 1% **1b** sample is clouded by inertial effects and not considered here). The apparent relaxation time (τ) of the samples with **1b** at different strains were obtained from the crossover frequency (ω_c) of G' and G'' during an oscillatory frequency sweep from 10 to 30 rad/s at three different applied strains ($\tau = 1 / \omega_c$) (Figures S6−S9 in the Supporting Information).[18] In the linear regime, τ is constant, while in the strain hardening regime, τ increases with strain. The increasing τ during strain hardening is consistent with the observed decrease in the phase angle, supporting a mechanism of an increasing number of elastically active chains.[18]

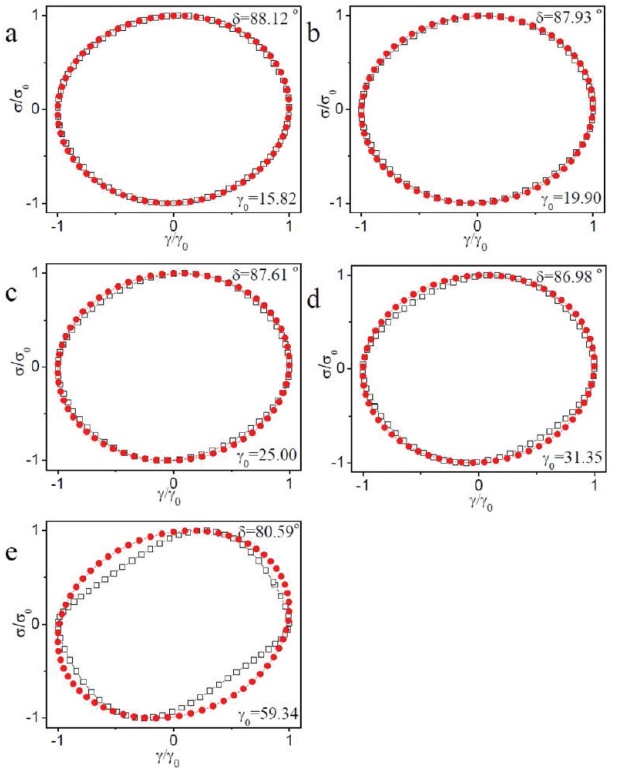

Figure 16. Normalized stress versus strain (Lissajous−Bowditch curves) for the raw data of ~0.11 g/mL PVP with 1% **1b** during strain sweep from the critical strain (γ_{crit}) to the maximum strain (γ_{max}) associated with strain hardening. The phase angle (δ) at different strains (γ_0) is shown. Unfilled square symbol represents the raw data. Filled circle symbols represent fits to the data assuming that time-dependent strain and stress are both single-harmonic sinusoids. The raw phase angle from the experiments is used in the fits. Scanning frequency is 1 rad/s.

In Figure 16, the Lissajous−Bowditch curves from the critical strain (γ_{crit}) to maximum strain (γ_{max}) during strain hardening of ~0.11 g/mL PVP with 1% **1b** are shown (scanning frequency is 1 rad/s). In Figure 16, we notice that, for $\gamma > \gamma_{crit}$, the phase angle decreases with increasing strain. At and just beyond the onset of strain hardening (Figure 16a,b), the Lissajous−Bowditch curves are elliptical. With further increases in strain (Figure 16c−e), the phase angle continues to decrease, but the Lissajous−Bowditch curves deviate increasingly from a clean ellipse. In comparison, the Lissajous−Bowditch curves for a

dx.doi.org/10.1021/ma201386t |Macromolecules 2011, 44, 7478–7488

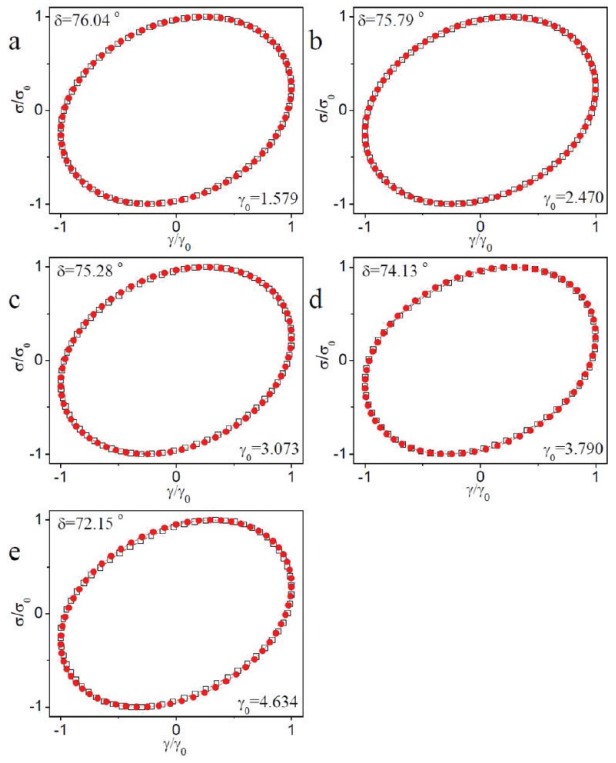

Figure 17. Normalized stress versus strain (Lissajous−Bowditch curves) for the raw data of ∼0.11 g/mL PVP with 5% **1b** during strain sweep from the critical strain (γ_{crit}) to the maximum strain (γ_{max}) associated with strain hardening. The phase angle (δ) at different strains (γ_0) is shown. Unfilled square symbol represent the raw data. Filled circle symbols represent fits to the data assuming that time-dependent strain and stress are both single-harmonic sinusoids. The raw phase angle from the experiments is used in the fits. Scanning frequency is 1 rad/s.

similar sample but with 5% **1b** deviate substantially from ellipticity only at the maximum strain (Figure 17), and similar behavior is observed for the sample with 2−4% **1b** (Figures S10−S12 in the Supporting Information), as is the case for the 5% **1b** sample at 30 rad/s (Figure S13 in the Supporting Information).

From the above data, an increase in τ and a decrease in the phase angle during strain hardening is observed, and we can infer that the primary mechanism underlying strain hardening is a strain-induced increase in the number of elastically active chains. At sufficiently large strains (i.e., just prior to network rupture), however, nonellipticity in the Lissajous−Bowditch curves is often observed. The apparent nonellipticity means that non-Gaussian stretching of polymer chains might also contribute to the strain hardening. Because nonellipticity of the Lissajous−Bowditch curves can also arise from other effects, including, for example, secondary flow or wall slip,[24,35,36] the loss of ellipticity alone cannot be taken as conclusive evidence for the non-Gaussian stretching of polymer chains. As polymer chains will be stretched when the Weissenberg number ($W_i = \gamma_0\omega\tau$) is larger than 1,[37] the value of the Weissenberg number at the maximum strain (γ_{max}) during strain hardening is also used to evaluate the contribution of the non-Gaussian stretching of polymer chains on strain hardening. The characterization of the apparent relaxation time (τ) of ∼0.11 g/mL PVP with 1% **1b** is shown in Figure S14 in the Supporting Information. The apparent relaxation time (τ) of ∼0.11 g/mL PVP with 1% **1b** in the linear regime is determined to be 1.1×10^{-2} s. From the data in Figure 15, we can see that the apparent relaxation times (τ) of the samples in the strain hardening regime are on the same order as that in the linear regime. We, therefore, assume that the value of τ of ∼0.11 g/mL PVP with 1% **1b** in the linear regime is close to the value of the apparent relaxation times (τ) of ∼0.11 g/mL PVP with 1% **1b** in the strain hardening regime and use this value to calculate the Weissenberg number ($W_i = \gamma_0\omega\tau$). For the strain sweep of ∼0.11 g/mL PVP with 1% **1b** at 1 rad/s, W_i is about 0.6 at the maximum strain (γ_{max}) during strain hardening (Figure 16e). This number is somewhat ambiguous, given the uncertainty in τ and the heterogeneous relaxation dynamics of these systems,[18] but because $W_i < 1$, non-Gaussian stretching of polymer chains is not obvious here,[37] and it is possible that the nonellipticity of the Lissajous−Bowditch curves is caused by other factors.[24,35,36] A similar picture emerges from an examination of the strain sweep behavior of ∼0.11 g/mL PVP with 5% **1b**. The data in Figure 4 reveal that W_i at γ_{max} ranges from 0.2 to 0.5 when $D_e < 1$ (scanning frequency ranges from 0.1 to 10 rad/s), while W_i at γ_{max} ranges from 0.9 to 1.3 when $D_e > 1$ (scanning frequency ranges from 20 to 30 rad/s). As W_i at γ_{max} during strain hardening is close to 1, and larger than 1 in some cases, contributions from the non-Gaussian stretching of polymer chains certainly cannot be excluded,[18,37] but quantifying the impact of any such effects is difficult.

For samples with 1% **1b** in the semidilute entangled PVP solution ([PVP] from 0.164 g/mL to 0.272 g/mL), τ is found to increase with strain during strain hardening (Figure S15 in the Supporting Information), consistent with the observed decrease in the phase angle, and the Lissajous−Bowditch curves of raw data are not elliptical only near γ_{max} (Figures S16−S19 in the Supporting Information). The same is true for samples with higher concentration of cross-linkers; for 0.259 g/mL PVP with 5% **1b**, τ increases (Figures S20−S23 in the Supporting Information), and the phase angle decreases during strain hardening. We infer that the primary mechanism of strain hardening in semidilute entangled solutions has the same increasing number of elastically active chains as in semidilute unentangled solutions.[18,23]

Absence of Strain Hardening in Semidilute Entangled Networks with Cross-Linker 1a. The purely strain softening behavior of G' and G'' for networks formed with cross-linker **1a** in the semidilute entangled regime, as opposed to the strain hardening observed for analogous samples formed with **1b** (Figures 9 and 10), implicates the contribution of a process whose dynamics are not strictly proportional to the lifetime of the cross-linkers. This behavior is reminiscent of the steady shear behavior reported previously for these networks, which similarly diverge.[23] The divergent behavior under steady shear was interpreted on the basis of a competition between two time scales: the average time that a cross-linker remains open (τ_1) and the local relaxation time of a polymer chain segment ($\tau_{segment}$).[23] For PVP networks with **1a** in DMSO at 25 °C, τ_1 is smaller than $\tau_{segment}$,[23] and entangled polymer strands do not have enough time to disentangle and then orient prior to reassociation. As a result, there is no net conversion of intrachain cross-linkers into elastically active interchain cross-linkers, and no shear thickening is observed.[23] The correspondence between shear thickening/thinning and strain hardening/softening in these networks as a function of the combination of cross-linker kinetics and PVP

concentration, coupled to the predominance of the shear- and strain-induced generation of elastically active subchains as the underlying mechanism for the observed shear thickening/strain hardening, strongly suggests that the same dynamic processes are operative in the divergent strain hardening/softening behavior reported here. We, therefore, infer that the absence of strain hardening in **1a**·PVP networks in the semidilute entangled regime is due to the fact that the average time that cross-linker **1a** remains open is too short to permit the local relaxation of polymer chain segments that is necessary for a net conversion of elastically inactive to elastically active cross-linkers.[23]

Absence of Strain Hardening in the Storage Moduli of 1b·PVP Networks in the Semidilute Entangled Regime. During steady shear, we previously observed shear thickening for **1b**·PVP in DMSO at 25 °C ($\tau_1 > \tau_{segment}$),[23] and in most cases, we observe analogous strain hardening in G' and G'' here. The strain sweep data for 0.259 g/mL PVP with 5% **1b** at 0.3 rad/s to 1 rad/s, however, reveals no strain hardening in G', although strain hardening is observed in G'' and $|G^*|$ (Figure 12). We interpret the absence of strain hardening in G' on the basis of eqs 4 and 5, which establish that, even within the same molecular mechanism, G' can fail to strain harden as a result of an increase in the phase angle (and associated decrease in $\cos(\delta)$) that is sufficient to counteract the increase due to complex modulus. Alternatively (or in addition), the strain hardening in G'' and $|G^*|$ could be attributed to non-Gaussian stretching. In Figures S24–S25 in the Supporting Information, however, there is at most only a small deviation from ellipticity in the relevant Lissajous–Bowditch curves for 0.259 g/mL PVP with 5% **1b** at 0.3 rad/s to 1 rad/s, and W_i is only about 0.3 before the break of the network. As the non-Gaussian stretching of polymer chains is not apparent here,[37] we cannot confirm that non-Gaussian stretching is the mechanism of strain hardening in G'' and $|G^*|$. The mechanism behind no strain hardening in G' and strain hardening in G'' and $|G^*|$ for 0.259 g/mL PVP with 5% **1b** at 0.3 rad/s to 1 rad/s is still an open question.

CONCLUSIONS

Strain hardening is observed under a large amplitude oscillatory shear (LAOS) of a family of metallo-supramolecular polymer networks. On the basis of accompanying variations of the phase angle and relaxation time, the strain hardening is attributed primarily to an increase in the number of elastically active chains, as opposed to non-Gaussian stretching of the polymer chains. Evidence for non-Gaussian stretching becomes apparent only at strains that are near that of network fracture, which must involve high degrees of polymer stretching in order to generate the forces necessary for rupture. These results present a unified picture of LAOS and steady shear behavior, as shear thickening in these networks has previously been associated with the same mechanism.

In the semidilute entangled regime of the PVP solution, samples with rapid cross-linker dissociation (k_d = 1450 s^{-1}) exhibit only strain softening (no strain hardening) for both the storage and loss moduli, in contrast to that of networks of identical equilibrium structure but slower cross-linkers (k_d = 17 s^{-1}). The strain softening of samples with faster cross-linkers is ascribed to the same mechanism previously reported for the pure shear thinning of networks with faster cross-linkers in the semidilute entangled regime; the average time that a cross-linker remains open (τ_1) is too short to permit the local relaxation of polymer chain segments ($\tau_{segment}$) that is necessary for a net conversion of elastically inactive to elastically active cross-linkers. Looking ahead, the mechanistic understanding of the nonlinear viscoelastic response of these networks provides a foundation for further work in which the LAOS behavior might be controlled through the rational molecular-scale design of supramolecular polymer networks. For example, one can envision optimizing the composition of these and related networks so that they strain harden to the maximum extent achievable for a given strain and strain rate.

ASSOCIATED CONTENT

Supporting Information. Lissajous–Bowditch curves of samples during strain hardening or strain softening; relaxation time (τ) of samples; relationship between strain hardening and the relaxation time of the network; variation in relaxation time during strain hardening. This material is available free of charge via the Internet at http://pubs.acs.org.

AUTHOR INFORMATION

Corresponding Author
*Email: dhxu@ciac.jl.cn (D.X.), stephen.craig@duke.edu (S.L.C.).

ACKNOWLEDGMENT

S.L.C. is thankful for the financial support by NSF (CHE-0646670) and NIH (EB-001037).

REFERENCES

(1) Berret, J. F.; Calvet, D.; Collet, A.; Viguier, M. *Curr. Opin. Colloid Interface Sci.* **2003**, *8*, 296–306.
(2) Pellens, L.; Corrales, R. G.; Mewis, J. *J. Rheol.* **2004**, *48*, 379–393.
(3) Marrucci, G.; Bhargava, S.; Cooper, S. L. *Macromolecules* **1993**, *26*, 6483–6488.
(4) Indei, T. *J. Non-Newtonian Fluid Mech.* **2007**, *141*, 18–42.
(5) Wang, S. Q. *Macromolecules* **1992**, *25*, 7003–7010.
(6) Witten, T. A., Jr.; Cohen, M. H. *Macromolecules* **1985**, *18*, 1915–1918.
(7) Hyun, K.; Kim, S. H.; Ahn, K. H.; Lee, S. J. *J. Non-Newtonian Fluid Mech.* **2002**, *107*, 51–65.
(8) Klucker, R.; Candau, F.; Schosseler, F. *Macromolecules* **1995**, *28*, 6416–6422.
(9) Ma, S. X.; Cooper, S. L. *Macromolecules* **2001**, *34*, 3294–3301.
(10) Tripathi, A.; Tam, K. C.; McKinley, G. H. *Macromolecules* **2006**, *39*, 1981–1999.
(11) Regalado, E. J.; Selb, J.; Candau, F. *Macromolecules* **1999**, *32*, 8580–8588.
(12) Tirtaatmadja, V.; Tam, K. C.; Jenkins, R. D. *Macromolecules* **1997**, *30*, 1426–1433.
(13) English, R. J.; Gulati, H. S.; Jenkins, R. D.; Khan, S. A. *J. Rheol.* **1997**, *41*, 427–444.
(14) Mewis, J.; Kaffashi, B.; Vermant, J.; Butera, R. J. *Macromolecules* **2001**, *34*, 1376–1383.
(15) Séréro, Y.; Jacobsen, V.; Berret, J. F.; May, R. *Macromolecules* **2000**, *33*, 1841–1847.
(16) Tan, H.; Tam, K. C.; Jenkins, R. D. *Langmuir* **2000**, *16*, 5600–5606.
(17) Albrecht, M.; van Koten, G. *Angew. Chem., Int. Ed.* **2001**, *40*, 3750–3781.
(18) Xu, D.; Hawk, J.; Loveless, D. M.; Jeon, S. L.; Craig, S. L. *Macromolecules* **2010**, *43*, 3556–3565.
(19) Loveless, D. M.; Jeon, S. L.; Craig, S. L. *Macromolecules* **2005**, *38*, 10171–10177.

(20) Yount, W. C.; Loveless, D. M.; Craig, S. L. *J. Am. Chem. Soc.* **2005**, *127*, 14488–14496.
(21) Xu, D.; Craig, S. L. *J. Phys. Chem. Lett.* **2010**, *1*, 1683–1686.
(22) Jeon, S. L.; Loveless, D. M.; Yount, W. C.; Craig, S. L. *Inorg. Chem.* **2006**, *45*, 11060–11068.
(23) Xu, D.; Liu, C. Y.; Craig, S. L. *Macromolecules* **2011**, *44*, 2343–2353.
(24) Ewoldt, R. H.; Hosoi, A. E.; McKinley, G. H. *J. Rheol.* **2008**, *52*, 1427–1458.
(25) Ewoldt, R. H.; McKinley, G. H. *Rheol. Acta* **2010**, *49*, 213–219.
(26) Hoy, R. S. *J. Polym. Sci., Part B: Polym. Phys.* **2011**, *49*, 979–984.
(27) Xu, D.; Craig, S. L. *Macromolecules* **2011**, *44*, 5465–5472.
(28) Chen, D.; Handa, H.; Wan, L.; Mao, G. *Macromol. Rapid Commun.* **2007**, *28*, 1619–1623.
(29) Loveless, D. M.; Jeon, S. L.; Craig, S. L. *J. Mater. Chem.* **2007**, *17*, 56–61.
(30) Franck, A. J. *Understanding Instrument Inertia Corrections in Oscillation*; TA Instruments: New Castle, DE , 2005.
(31) Ferry, J. D. *Viscoelastic Properties of Polymers*; John Wiley & Sons, Inc.: New York, 1980.
(32) Orakdogen, N.; Erman, B.; Okay, O. *Macromolecules* **2010**, *43*, 1530–1538.
(33) Erk, K. A.; Henderson, K. J.; Shull, K. R. *Biomacromolecules* **2010**, *11*, 1358–1363.
(34) Tung, S. H.; Raghavan, S. R. *Langmuir* **2008**, *24*, 8405–8408.
(35) Atalik, K.; Keunings, R. *J. Non-Newtonian Fluid Mech.* **2004**, *122*, 107–116.
(36) Graham, M. D. *J. Rheol.* **1995**, *39*, 697–712.
(37) Larson, R. G. *The Structure and Rheology of Complex Fluids*; Oxford University Press: New York, 1999.
(38) Yosick, J. A.; Giacomin, A. J. *J. Non-Newtonian Fluid Mech.* **1996**, *66*, 193–212.
(39) Tapadia, P.; Ravindranath, S.; Wang, S. Q. *Phys. Rev. Lett.* **2006**, *96*, 196001.
(40) Li, X.; Wang, S. Q.; Wang, X. R. *J. Rheol.* **2009**, *53*, 1255–1274.
(41) Bossard, F.; Sfika, V.; Tsitsilianis, C. *Macromolecules* **2004**, *37*, 3899–3904.
(42) Ma, L.; Yamada, S.; Wirtz, D.; Coulombe, P. A. *Nat. Cell Biol.* **2001**, *3*, 503–506.